AIAA JOURNAL
Vol. 35, No. 6, June 1997

Estimation of Aeroelastic Models in Structural Limit-Cycle Oscillations from Test Data

Szu-Ying Tan*
Aeronautical Research Laboratory, Taichung, Taiwan 40722, Republic of China
and
C. Edward Lan†
University of Kansas, Lawrence, Kansas 66045

An optimal estimation algorithm to identify aeroelastic models in structural limit-cycle oscillations (LCO) is developed. This algorithm is based on an optimal estimation theory with a continuous cost function to minimize the difference between the estimates and data. The optimality equations are reformulated in the frequency domain through Beecham–Titchener's averaging technique. The resulting equations are then solved by a finite difference method. A wing rock model of an 80-deg delta wing is used to verify the method. The method is then applied to the left engine nacelle of a jet transport airplane in structural LCO. Estimated system models include terms representing nonlinear stiffness and damping. On the basis of these estimated aeroelastic models, the necessary additional damping for LCO suppression can be computed. It is also shown that increasing the system stiffness alone may not eliminate the structural LCO.

Nomenclature

A, a	= amplitude function
$C_1 \sim C_3$	= coefficients in Eq. (1)
D_i	= coefficients of the estimated model equation
d_{11}	$= -\mu^2 + \omega^2 + C_1 - C_2\mu + 0.75C_3a^2$
d_{12}	$= 2\mu\omega + C_2\omega$
d_{21}	$= -2\mu\omega - C_2\omega$
d_{22}	$= -\mu^2 + \omega^2 + C_1 - C_2\mu - 2.25C_3a^2$
F, f	= forcing function
G	= implicit function
H	= Hamiltonian
h_1	$= 2\mu\omega - C_2\omega$
h_2	$= -\mu^2 + \omega^2 + C_1 + C_2\mu + 0.75C_3a^2$
J	= cost function
M	= Mach number
q	= displacement
t	= time
Δ	= residual
η	= out-of-phase part of the Lagrangian multiplier
θ	= angle
λ	= Lagrangian multiplier
μ	$= \dot{a}/a$
ξ	= in-phase part of the Lagrangian multiplier
ϕ	= roll angle
ω	= frequency

Introduction

A LIMIT-CYCLE oscillation (LCO) is a self-sustaining oscillation with a limited amplitude that occurs as a result of nonlinear coupling between the dynamic response and unsteady aerodynamic forces. Well-known examples of LCO in aircraft engineering are wing rock and structural LCO. A structural LCO is characterized by an almost harmonic oscillation, which has been shown to occur mostly in the transonic speed regime.[1] The analysis in Ref. 2 has indicated that the shock-induced trailing edge separation plays a dominant role in the development of structural LCO of an F-16A half-wing model at a transonic speed.

Because the flow conditions in LCO are characterized by a mixed attached/separated flow, such as the flowfield involving a shock–boundary layer interaction, theoretical prediction of the phenomenon is difficult. Reference 1 presented a semiempirical method for this purpose. Euler solutions were used in Ref. 3 to predict the structural LCO of an airfoil in the angle of attack and plunging modes. For a three-dimensional configuration, a current practice is to rely on experimental testing with a dynamically scaled model.[4] In testing, it is useful to determine the forcing function for the purpose of later simulation.

There has been a constant effort in determining the aeroelastic models that cause LCO from flight test or wind-tunnel measurement. The primary difficulty in identification of aeroelastic models lies in the nonlinear characteristics of the dynamic system. The existing parameter estimation methods, such as the equation error method,[5] output error method,[6,7] and maximum-likelihood method,[8] or a combination of some of these methods,[9] have been applied in the past mainly to estimating the aircraft aerodynamic parameters in relatively slow motions. Some common features of these methods are the assumption of aerodynamic model structure and minimization of cost function in the time domain. The nonlinear system identification technique employed in Ref. 10 to investigate the LCO was based on the bispectral signal processing, and aeroelastic models have not been specifically identified.

The objective of this paper is to present a model estimation method based on minimizing a continuous cost function without assuming a model structure in estimating the forcing function. The optimality equations are solved in the frequency domain to take advantage of the fact that the system frequency in LCO is nearly constant. Application to the structural LCO of an engine nacelle is then presented.

Theoretical Development

Derivation of Governing Equations

Because the LCO is primarily a single-degree-of-freedom oscillation, a scalar equation will be used to illustrate the derivation. The equation of motion is written in a state variable form with q being the displacement, as

$$\begin{aligned} \dot{q} &= v \\ \dot{v} &= F(t) = C_1 q + C_2 \dot{q} + C_3 q^3 + f(t) \end{aligned} \tag{1}$$

with initial conditions

$$q(0) = q_0 \qquad v(0) = v_0$$

Received July 5, 1996; revision received Feb. 10, 1997; accepted for publication Feb. 25, 1997.

*Supervisor, Aerodynamics Department, P.O. Box 90008-11-1.

†Bellows Distinguished Professor, Department of Aerospace Engineering. Associate Fellow AIAA.

In Eq. (1), $f(t)$ can be viewed as a control function to be determined by an optimal control theory subject to the constraint of satisfying the dynamic equation (1). The coefficients $C_1 \sim C_3$ will be assumed in the estimation process to help numerical convergence, as will be shown later. The forcing function $F(t)$ is calculated as a function of t.

Assume that $q_d(t)$ represents the measured LCO response. The forcing function $f(t)$ is to be determined to produce a system response to match $q_d(t)$ as closely as possible, taking possible measurement uncertainties into account. So the problem at hand is a tracking problem in optimal control theory. The forcing function is obtained by forcing the displacement and velocity to follow the specified $q_d(t)$ and $\dot{q}_d$. So the cost function to be minimized is defined as

$$J = \frac{1}{2}\int_0^{t_f} \left[(\dot{q} - \dot{q}_d)^2 + (q - q_d)^2 + f^2\right] \mathrm{d}t \tag{2}$$

To minimize the cost function [Eq. (2)] subject to the constraint [Eq. (1)], the following Hamiltonian must be optimized:

$$H = (\dot{q} - \dot{q}_d)^2 + (q - q_d)^2 + f^2 + \lambda_1 v + \lambda_2(C_1 q + C_2\dot{q} + C_3 q^3 + f) \tag{3}$$

$$\lambda_1(t_f) = 0 \qquad \lambda_2(t_f) = 0$$

where λ_1 and λ_2 are the Lagrangian multipliers. The necessary optimality conditions, in addition to Eq. (1), are

$$\dot{\lambda}_1 = -\frac{\partial H}{\partial q} = -2(q - q_d) - C_1\lambda_2 - 3C_3\lambda_2 q^2 \tag{4}$$

$$\dot{\lambda}_2 = -\frac{\partial H}{\partial v} = -2(\dot{q} - \dot{q}_d) - \lambda_1 - C_2\lambda_2 \tag{5}$$

$$\frac{\partial H}{\partial f} = 2f + \lambda_2 = 0 \tag{6}$$

From Eq. (6), the forcing function $f(t)$ can be obtained as

$$f = -\lambda_2/2 \tag{7}$$

Equations (1), (4), and (5) are coupled nonlinear equations with initial conditions for q and final conditions ($t \to \infty$) for λ_1 and λ_2. Because the conditions are imposed at two different points, these equations cannot be easily integrated. For a two-point boundary-value problem, "flooding" or "successive linearization"[11] is a possible way to obtain the solution. However, in integration with these schemes, the solution is very sensitive to a small change in the unspecified initial conditions. Therefore, long computational time is expected even if the solution converges. For the present purpose, we first reduce these equations to the frequency domain by Beecham–Titchener's method[12] (B–T method) and eliminate λ_1 and λ_2 from the resulting equations. The B–T method has been used successfully in the past.[13]

B–T Method

Periodic motions can be expressed by pure sinusoidal functions. Assume a trial solution in the form of

$$q = a\cos\theta \tag{8}$$

where both a and θ are functions of t. The solution of Lagrangian multipliers is expected to consist of an in-phase part (i.e., $\cos\theta$ term) and an out-of-phase part (i.e., $\sin\theta$ term), so the following forms for λ_1 and λ_2 are assumed:

$$\lambda_1 = a(\xi_1 \sin\theta + \eta_1 \cos\theta) \tag{9}$$

$$\lambda_2 = a(\xi_2 \sin\theta + \eta_2 \cos\theta) \tag{10}$$

where a, θ, ξ_1, η_1, ξ_2, and η_2 are functions of t. Differentiating Eqs. (8–10), we obtain

$$\dot{q} = a(\mu\cos\theta - \omega\sin\theta) \tag{11}$$

$$\ddot{q} = a[(\mu^2 - \omega^2 + a\mu\mu')\cos\theta - (2\mu\omega + a\mu\omega')\sin\theta] \tag{12}$$

$$\dot{\lambda}_1 = a\{[\mu(\eta_1 + a\eta_1') + \omega\xi_1]\cos\theta + [\mu(\xi_1 + a\xi_1') - \omega\eta_1]\sin\theta\} \tag{13}$$

$$\dot{\lambda}_2 = a\{[\mu(\eta_2 + a\eta_2') + \omega\xi_2]\cos\theta + [\mu(\xi_2 + a\xi_2') - \omega\eta_2]\sin\theta\} \tag{14}$$

where $\mu = \dot{a}/a$, $\omega = \dot{\theta}$, and $(\,)' = \mathrm{d}(\,)/\mathrm{d}a$. As a first approximation, it is assumed in accordance with the B–T method that

$$\mu' = \omega' = \xi_1' = \eta_1' = \xi_2' = \eta_2' = 0$$

Substituting Eqs. (8), (11), and (12) into Eq. (1), the following two equations are obtained by the harmonic averaging method[13]:

$$\mu^2 - \omega^2 = C_1 + C_2\mu + \tfrac{3}{4}C_3 a^2 - \eta_2/2 \tag{15}$$

$$2\mu\omega = C_2\omega + \xi_2/2 \tag{16}$$

To eliminate λ_1 and λ_2, we first obtain from Eqs. (4), (8), (11), and (13),

$$(\mu\xi_1 - \omega\eta_1 + C_1\xi_2)\sin\theta + (\mu\eta_1 + \omega\xi_1 + 2 + C_1\eta_2)\cos\theta = 2(q_d/a) - 3C_3a^2\eta_2\cos^3\theta - 3C_3a^2\xi_2\cos^2\theta\sin\theta \tag{17}$$

In Eq. (17), $q_d(t)$ is known. To apply the averaging method, $q_d(t)$ must be expressed in terms of $\sin\theta$ and $\cos\theta$. Therefore, q_d is taken to be

$$q_d = A(t)\cos\theta \tag{18}$$

A and $\dot{A}$ can be obtained by differentiating Eq. (18):

$$A = q_d/\cos\theta \tag{19}$$

$$\dot{A} = \dot{q}_d/\cos\theta + \omega q_d \sin\theta/\cos^2\theta \tag{20}$$

Equation (17) is again separated into the in-phase and out-of-phase parts by harmonic averaging:

$$\mu\eta_1 + \omega\xi_1 = -2(1 - A/a) - (C_1 + 2.25C_3a^2)\eta_2 \tag{21}$$

$$\mu\xi_1 - \omega\eta_1 = -(C_1 + 0.75C_3a^2)\xi_2 \tag{22}$$

Similarly, substituting Eqs. (8), (11), (14), and (18) into Eq. (5) and applying the averaging method give

$$\xi_1 = 2\omega(1 - A/a) - (\mu + C_2)\xi_2 + \omega\eta_2 \tag{23}$$

$$\eta_1 = -2(\mu - \dot{A}/a) - (\mu + C_2)\eta_2 - \omega\xi_2 \tag{24}$$

Equations (23) and (24) can be used to eliminate ξ_1 and η_1 from Eqs. (21) and (22). It follows that

$$(\omega^2 - \mu^2 + C_1 - C_2\mu + 0.75C_3a^2)\xi_2 + (2\mu\omega + C_2\omega)\eta_2 = -2\mu\omega(1 - A/a) - 2\omega(\mu - \dot{A}/a) \tag{25}$$

$$(-2\mu\omega - C_2\omega)\xi_2 + (\omega^2 - \mu^2 - C_2\mu + 2.25C_3a^2 + C_1)\eta_2 = -2(1 + \omega^2)(1 - A/a) + 2\mu(\mu - \dot{A}/a) \tag{26}$$

In Eqs. (25) and (26), there are still terms representing the effect of Lagrangian multipliers (i.e., ξ_2 and η_2). To eliminate these, Eqs. (15) and (16) are solved for ξ_2 and η_2 to give

$$\xi_2 = 2(2\mu\omega - C_2\omega) \tag{27}$$

$$\eta_2 = 2(\omega^2 - \mu^2 + C_1 + C_2\mu + 0.75C_3a^2) \tag{28}$$

Substituting ξ_2 and η_2 into Eqs. (25) and (26) gives

$$d_{11}h_1 + d_{12}h_2 = -\mu\omega(1 - A/a) - \omega(\mu - \dot{A}/a) \tag{29}$$

$$d_{21}h_1 + d_{22}h_2 = -(1 + \omega^2)(1 - A/a) + \mu(\mu - \dot{A}/a) \tag{30}$$

In these final equations to be solved, Eqs. (29) and (30), the Lagrangian multipliers, ξ_1, η_1, ξ_2, and η_2, have all been eliminated.

Because $\mu = \dot{a}/a$, $\omega = \dot{\theta}$, Eqs. (29) and (30) represent a set of nonlinear implicit ordinary differential equations of the form

$$G(y', y) = 0 \tag{31}$$

where G is a two-dimensional function, $y' = (\dot{a}, \dot{\theta})$, $y = (a, \theta)$, and the initial conditions a_0 and θ_0 can be obtained from q_0 and v_0. Equation (31) with specified initial conditions can be solved by an existing code DASSL[14] with a backward difference formulation.

Summary of the Present Method

The resulting optimal estimation equations, Eqs. (29) and (30), are integrated for $a(t)$ and $\theta(t)$. From Eqs. (27) and (28), ξ_2 and η_2 are then determined. From Eqs. (7) and (10), the estimated forcing function is obtained:

$$f(t) = -(a/2)(\xi_2 \sin\theta + \eta_2 \cos\theta) \tag{32}$$

The total forcing function $F(t)$ is the sum of C terms and $f(t)$. Finally, a model equation is assumed for $F(t)$. For this purpose, the approaches of the Volterra series[15] and indicial integrals through Fourier functional analysis[16] may be used. Both approaches account for the time history effect in aerodynamics. Theoretically, a Volterra series represents an asymptotic expansion for the solution with respect to system nonlinearity. Identification of its high-order kernels is considered to be difficult. Yet in one application to wing rock LCO, a series of more than fourth order is needed to obtain the correct amplitude.[17] Besides, the first-order, or linear, Volterra integral does not incorporate the memory effect,[15] whereas in unsteady aerodynamics the time history effect is significant even in linear theory. Therefore, based on an aerodynamic consideration a proper choice is the indicial integral approach of Ref. 16. In the frequency domain, this approach can be viewed through Fourier transform as obtaining a model equation with coefficients as functions of frequency. Because LCO is the response with a single dominant frequency, for all practical purposes the model can be assumed to consist of nonlinear algebraic expressions of the following form:

$$F(t) = D_1 q + D_2 \dot{q} + D_3 \dot{q}|q| + D_4 \dot{q}|\dot{q}| + D_5 q^2 + D_6 q^3 + \ldots \tag{33}$$

where the nonanalytic terms associated with the absolute values are introduced to reduce the number of necessary terms in the model and have been verified in wing rock LCO.[13,18]

The computational algorithm is as follows.

1) The starting time in the test data to be used is typically one at which the reading is at a peak (i.e., the initial point is at a peak of a cosine curve).

2) The amplitude A at any time t is obtained by using successive peak values and the corresponding times. Within these time intervals, the amplitude A at any time t is obtained by Lagrange's interpolation method.

3) The time rate of change in amplitude $\dot{A}$ is calculated by numerical differentiation with a second-order central difference scheme. The scheme is based on an uneven spacing.

4) The lapse between two successive peaks represents a local period of the oscillation. The reciprocal of the period is the local frequency. The frequency ω_l at any time t is then obtained by interpolation of these local frequency data. A fast Fourier transform program, DFT, can also be used to find ω_l.

5) C_1 in Eqs. (29) and (30) is set equal to $-\omega_l^2$, and $C_2 = 2\dot{A}/A$ when the DASSL program is used to integrate Eqs. (29) and (30).

6) The initial values a_0, $\dot{a}_0$, θ_0, and ω_0 for the integration in DASSL should be consistent, i.e., they must satisfy the implicit differential equations. The values obtained in steps 3 and 4 may be used as the initial trial values.

Numerical Results and Discussion

The present estimation algorithm will be verified with a specific mathematical model for wing rock of an 80-deg delta wing.[13,18] After verification, the present method will be applied to the left engine nacelle of a jet transport airplane in limit cycle oscillations.

80-deg Delta Wing

For the 80-deg delta wing, the time history data of roll angle were generated through Runge–Kutta numerical integration of the following wing rock model equation:

$$\ddot{\phi} = -26.6667\phi + 0.76485\dot{\phi} - 2.92173\dot{\phi}|\phi| \tag{34}$$

It is found that by setting $C_1 = -\omega_l^2$, $C_2 = 2\dot{A}/A$, and $C_3 = 0$, the present scheme would converge well. A fixed-error tolerance $= 10^{-6}$ and $\Delta t = 0.025$ in DASSL would produce the following reasonable results[19]:

$$\ddot{\phi} = -26.592\phi + 0.741\dot{\phi} - 2.826\dot{\phi}|\phi|$$

To improve, Δt must be reduced to result in increased computing time. For example, if $\Delta t = 0.005$, the estimated coefficients would agree with those in Eq. (34) to within 0.1%. In the following application, Δt will be set to 0.025.

Lateral Oscillation of the Left Engine Nacelle of a Jet Transport Airplane

The flight test data were obtained at $M = 0.894$ and an altitude of 22,000 ft (6705.6 m). The test data cover approximately 40 s of level flight. The program DFT was used to find the frequency contents in the test data and the dominant frequency component. This frequency was used to determine the constant C_1 in Eq. (1). For the present case, the algorithm will not converge if C_3 in Eq. (1) is set to zero. Through numerical experimentation, setting C_3 to any value of order one will work well. In the following, C_3 is always set to 1.

Test data for the lateral oscillation are presented in Fig. 1. The estimated forcing function is shown in Fig. 2. Just like Fourier analysis of any function, this estimated forcing function can be fitted

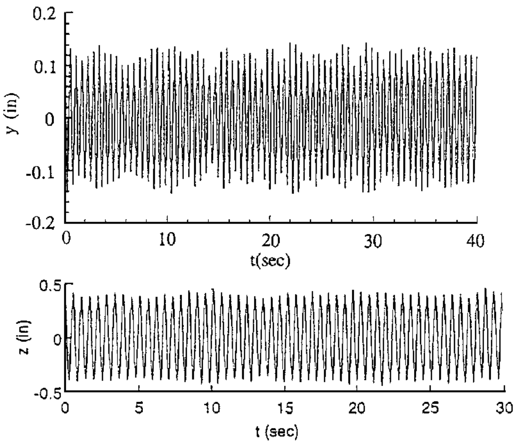

Fig. 1 Lateral and vertical oscillations of an engine nacelle of a jet transport; $M = 0.894$ and altitude = 22,000 ft (6705.6 m).

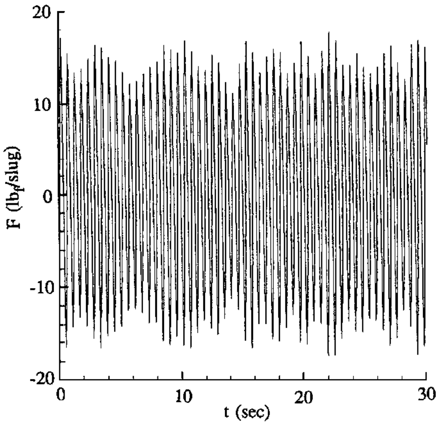

Fig. 2 Estimated forcing function in lateral oscillation of an engine nacelle; $M = 0.894$, altitude = 22,000 ft (6705.6 m), and 1 lbf per slug = 0.3048 N/kg.

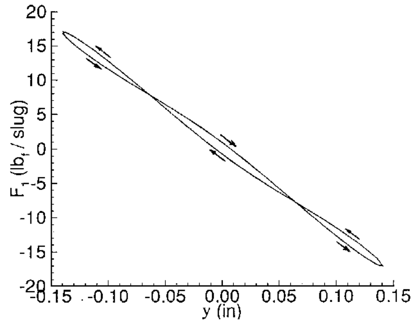

Fig. 3 Hysteresis loops in the lateral LCO of an engine nacelle based on the estimated aeroelastic model.

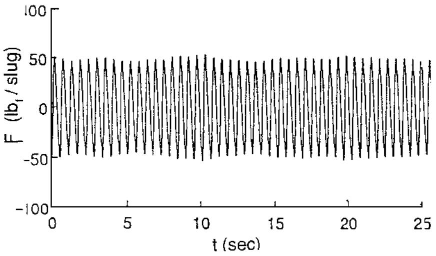

Fig. 4 Estimated forcing function in the vertical LCO of an engine nacelle; $M = 0.894$, altitude = 22,000 ft (6705.6 m), and 1 lbf per slug = 0.3048 N/kg.

successively with modes of different frequencies. The first mode is estimated to be

$$F_1(t) = -124.404 y_1 + 1.869 \dot{y}_1 - 17.833 \dot{y}_1 |y_1| - 2.358 \dot{y}_1 |\dot{y}_1| + 2.803 y_1^2 - 388.175 y_1^3 \tag{35}$$

The estimated force is well-fitted with this model with a least-squares error of 1.77×10^{-5}. The agreement of mode 1 response with the original test data can be shown to be reasonable.[19]

The estimated model [Eq. (35)] consists of a relatively large negative linear damping ($1.869\dot{y}_1$) but has positive nonlinear damping. This means the response will achieve the steady amplitude quickly when the system is disturbed. The hysteresis loops shown in Fig. 3 are similar to the wing rock LCO. There are three loops, two counterclockwise (energy dissipating) and one clockwise (energy gaining). From the viewpoint of energy balance, the energy gained in the center loop is balanced by the energy dissipated in the two neighboring counterclockwise loops.

Vertical Oscillation of the Left Engine Nacelle of a Jet Transport Airplane

Test data for the vertical oscillation are also presented in Fig. 1. The estimated forcing function is presented in Fig. 4. The first model is given by

$$F_1(t) = -124.25 z_1 + 0.007 \dot{z}_1 - 0.017 \dot{z}_1 |z_1| - 0.002 \dot{z}_1 |\dot{z}_1| + 0.011 z_1^2 - 0.014 z_1^3 \tag{36}$$

The estimated force was also fit with polynomials of different degrees, up to the fifth. The calculated responses with these higher-degree polynomials do not show much improvement.[19]

Application of Estimated Aeroelastic Models

Once the aeroelastic model is estimated, the same model can be used in improving the system response as long as the aerodynamic configuration remains the same. The estimated aeroelastic models can be used to determine the aerodynamic models if the structural models are known. Examples of system modifications to improve the response are the design of feedback control and structural modifications. In the application to a control system design, mechanical or artificial damping of different values can be added to the estimated model to improve the behavior of system response. Model simulation provides an idea about how much damping and stiffness are needed.

In the present application to nacelle oscillation in the absence of structural models, we may estimate based on an aerodynamic consideration that most of the displacement effect comes from the structural stiffness and the velocity terms from the aerodynamic effect. Based on this assumption, the effect of changing stiffness and damping on the lateral oscillation is numerically simulated.[19] When $D_1 = -124.404$ [Eq. (35)] is changed to -2×124.404 (increasing linear stiffness), the system response frequency is increased and the amplitude is reduced. However, LCO cannot be eliminated. On the other hand, if $D_2 = 1.869$ is changed to -1.869 (i.e., positive damping), the lateral LCO is damped quickly.

For the vertical oscillation, the response amplitude is not altered by changing $D_1 = -124.25$ [Eq. (36)] to -2×124.25 as in the case of lateral oscillation. Again, a negative D_2 value can damp out the LCO.

Because the dynamic system often consists of an assembly of structural parts, nonlinearities in stiffness may exist to cause the LCO. To see this possibility, the estimated models are again used as follows. For the lateral oscillation, if the nonlinear stiffness terms are assumed zero (i.e., $D_5 y^2$, $D_6 y^3$ terms), the response is found not being much affected. On the other hand, by setting the nonlinear damping terms (i.e., $D_3 \dot{y}|y|$, $D_4 \dot{y}|\dot{y}|$ terms) to zero, the response amplitude is increased as expected. For the vertical oscillation, having the coefficients of the nonlinear stiffness terms, D_5 and D_6, being zero does not significantly affect the system response. In addition, setting D_3 and D_4 to zero does not affect the system response either. The reason is probably that the coefficients D_3 and D_4 are already small. Based on these simulation results, it can be concluded that factors other than structural nonlinearity, such as nonlinear aerodynamic damping, are responsible for the occurrence of LCO.

Conclusions

A method to estimate the aerodynamic forcing function in LCO of aerodynamic configurations has been developed. The method was based on an optimal estimation theory in the frequency domain. The present method used a continuous cost function that was a measure of the difference between the estimated states and the measured data. Simplification of the optimality equations through the B–T averaging method allowed the Lagrangian multipliers to be eliminated from the equations to be solved. The forcing function thus obtained was fitted with state variables and their products through a least-squares method.

The current method was verified with a wing rock model for an 80-deg delta wing and then used to estimate the forcing functions of an engine nacelle of a jet transport in lateral and vertical oscillations. The model simulations were compared with the measured data with fair agreement. The estimated models exhibited an odd number of hysteresis loops.

Possible applications of the estimated aeroelastic models were illustrated. The model simulation illustrated the sensitivity of the system response to various parameter values. It was shown that adding damping would damp the LCO as expected. The amount of damping needed to damp out the LCO could be determined by the present estimated aeroelastic models. For the engine nacelle, adding a reasonable amount of stiffness alone was shown to be unable to eliminate the LCO in the simulation.

References

[1] Meijer, J., and Cunningham, A., Jr., "Understanding and Development of a Prediction Method of Transonic Limit-Cycle Oscillation Characteristics of Fighter Aircraft," AIAA Paper 92-4501, Aug. 1992.

[2] Cunningham, A. M., Jr., and der Boer, R. G., "Transonic Wind Tunnel Investigation of Limit Cycle Oscillations on Fighter Type Wings," AGARD-CP-507, March 1992.

[3] Kousen, K. A., and Bendiksen, O. O., "Limit Cycle Phenomena in Computational Transonic Aeroelasticity," *Journal of Aircraft*, Vol. 31, No. 6, 1994, pp. 1257–1263.

[4] Seidel, D. A., Eckstrom, C. V., and Sandford, M. C., "Transonic Region of High Dynamic Response Encountered on an Elastic Supercritical Wing," *Journal of Aircraft*, Vol. 26, No. 9, 1989, pp. 870–875.

[5]Aksteter, J. W., Parks, E. K., and Bach, R. E., Jr., "Parameter Identification and Modeling of Longitudinal Aerodynamics," *Journal of Aircraft*, Vol. 32, No. 4, 1995, pp. 726–731.

[6]Maine, R. E., and Iliff, W. K., "Application of Parameter Estimation to Aircraft Stability and Control—The Output-Error Approach," NASA Reference Publication 1168, June 1986.

[7]Preissler, H., and Schäufele, H., "Equation Decoupling—A New Approach to the Aerodynamic Identification of Unstable Aircraft," *Journal of Aircraft*, Vol. 28, No. 2, 1991, pp. 146–150.

[8]Iliff, K. W., and Maine, R. E., "Maximum Likelihood Estimation with Emphasis on Aircraft Flight Data," *JPL Proceedings of the Workshop on Identification and Control of Flexible Space Structures*, Vol. 3, Jet Propulsion Lab., California Inst. of Technology, Pasadena, CA, 1985, pp. 197–246.

[9]Trankle, T. L., and Bachner, S. D., "Identification of a Nonlinear Aerodynamic Model of the F-14 Aircraft," *Journal of Guidance, Control, and Dynamics*, Vol. 18, No. 6, 1995, pp. 1292–1297.

[10]Stearman, R. O., Powers, E. J., Schwartz, J., and Yurkovich, R., "Aeroelastic System Identification of Advanced Technology Aircraft Through Higher Order Signal Processing," *Proceedings of the 9th International Modal Analysis Conference* (Florence, Italy), Pt. 2, Society for Experimental Mechanics, Bethel, CT, 1991, pp. 1607–1615.

[11]Citron, S. J., *Element of Optimal Control*, Holt, Rinehart, and Winston, New York, 1969, pp. 109–112.

[12]Beecham, L. T., and Titchener, I. M., "Some Notes on an Approximate Solution for the Free Oscillation Characteristics of Non-Linear System Typified by $\ddot{X} + F(X, \dot{X}) = 0$," British Aeronautical Research Council, Repts. and Memoranda 3651, London, Aug. 1969.

[13]Luo, J., and Lan, C. E., "Control of Wing-Rock Motion of Slender Delta Wings," *Journal of Guidance, Control, and Dynamics*, Vol. 16, No. 2, 1993, pp. 225–231.

[14]Brenan, K. E., Campbell, S. L., and Petzold, L. R., *Numerical Solution of Initial-Value Problem in Differential-Algebraic Equations*, Elsevier Science, New York, 1989, pp. 115–148.

[15]Silva, W. A., "Application of Nonlinear Systems Theory to Transonic Unsteady Aerodynamic Responses," *Journal of Aircraft*, Vol. 30, No. 5, 1993, pp. 660–668.

[16]Lan, C. E., Chen, Y., and Lin, K. J., "Experimental and Analytical Investigation of Transonic Limit-Cycle Oscillations of a Flaperon," *Journal of Aircraft*, Vol. 32, No. 5, 1995, pp. 905–910.

[17]Baumann, W. T., Herdman, T. O., Stalford, H. L., and Garrett, F. E., "A Volterra Series Submodel Approach to Modeling Nonlinear Aerodynamics Systems," U.S. Air Force Flight Dynamics Lab., AFWAL-TR-88-3040, Wright–Patterson AFB, OH, May 1988.

[18]Nguyen, L.T., Yip, L., and Chambers, J. R., "Self-Induced Wing Rock of Slender Delta Wings," AIAA Paper 81-1883, Aug. 1981.

[19]Tan, S. Y., "Identification of Aerodynamic Models in Limit-Cycle Oscillations," Ph.D. Dissertation, Dept. of Aerospace Engineering, Univ. of Kansas, Lawrence, KS, Jan. 1996.

R. W. Wlezien
Associate Editor